DOI 10.1007/s11182-017-1133-4

Russian Physics Journal, Vol. 60, No. 4, August, 2017

ERRATUM

To the article "Peculiarities of pair creation by a peak electric field" by T. C. Adorno, S. P. Gavrilov, D. M. Gitman and R. Ferreira, Vol. 60, No. 3, pp. 417–426, 2017.

An acknowledgement is made that does not correspond to the article. Therefore, the final paragraph of the article on page 425, namely, "This work was supported in part by the USA Energy Department (Contract DE-AC-02-76SF00515. SLACPUB-16913)" should be replaced by "The research was supported by the Russian Science Foundation (Grant No. 15-12-10009)."

DOI 10.1007/s11182-017-1090-y
Russian Physics Journal, Vol. 60, No. 3, July, 2017 (Russian Original No. 3, March, 2017)

PECULIARITIES OF PAIR CREATION BY A PEAK ELECTRIC FIELD

T. C. Adorno,[1] S. P. Gavrilov,[1,2] D. M. Gitman,[1,3,4] and R. Ferreira[4]

UDC 530.22

*Exact, numerical, and asymptotic calculations concerning the vacuum instability by the so-called peak electric field are explored in detail. Peculiarities discussed in this article are complementary to those published recently by us in Eur. Phys. J. C, **76**, p. 447 (2016), in which the effect was studied in the framework of QED with t-electric potential steps. To discuss features beyond the asymptotic regime, we present numerical details of exact and asymptotic expressions inherent to the peak field and discuss differential and total quantities. The results show wider distributions, with respect to the longitudinal momentum, as the phases k_1 and k_2 of the electric field decrease and larger distributions as the amplitude E increases. Moreover, the total density of pairs created decreases as k_1 and k_2 increase, its dependence being proportional to k_1^{-1} and k_2^{-1}. The latter result is more accurate as k_1 and k_2 decrease and confirms, in particular, our asymptotic estimates obtained previously.*

Keywords: QED with external fields, particle creation, Dirac equation.

INTRODUCTION

Vacuum instability by external fields is a pure quantum effect whose description is entirely nonperturbative. In quantum electrodynamics (QED), for instance, the phenomena are characterized by the materialization of electron-positron pairs from the vacuum and, by virtue of this process, the vacuum itself becomes unstable. The problem has an old origin whose history has been formed by an extensive list of contributions, initiated mostly after the works of Klein [1], Sauter [2], Heisenberg and Euler [3], and Hund [4] and developed years ahead, for example, by Schwinger [5], Furry [6], Nikishov, Narozhny, and Ritus [7–13], Brezin and Itzykson [14], Popov [15], and Gitman and Fradkin [16, 17] among others. For a detailed discussion on the problem and a relevant list of publications, see [18–23] or some reviews [24, 25].

In this article we summarize the main aspects of particle creation from the vacuum by a peak electric field [26] and present new details on differential mean number of particles created as well as total quantities.

[1]National Research Tomsk State University, Tomsk, Russia, e-mail: adorno@phys.tsu.ru; gavrilovsergeyp@yahoo.com; [2]Herzen State Pedagogical University of Russia, Saint Petersburg, Russia, e-mail: gavrilovsp@herzen.spb.ru; [3]P. N. Lebedev Physical Institute of the Russian Academy of Sciences, Moscow, Russia; [4]Institute of Physics of the University of São Paolo, São Paolo, Brazil, e-mail: gitman@if.usp.br. Translated from Izvestiya Vysshikh Uchebnykh Zavedenii, Fizika, No. 3, pp. 37–45, March, 2017. Original article submitted December 23, 2016.

1. PAIR CREATION BY A PEAK ELECTRIC FIELD

We remind that the peak electric field is an example of a t-electric potential step [21] characterized by a time-dependent electric field directed along a unique direction[1]

$$\boldsymbol{E}(t)=\left(E^{i}(t)=\delta_{1}^{i}E(t),\ i=1,...,D\right), \tag{1}$$

provided by a vector potential in the gauge

$$A^{0}=0,\ \boldsymbol{A}(t)=\left(A^{i}(t)=\delta_{1}^{i}A_{x}(t)\right),$$

$$\dot{A}_{x}(t)=\frac{dA_{x}(t)}{dt}\leq 0\rightarrow\begin{cases}E(t)=-\dot{A}_{x}(t)\geq 0,\\ A_{x}(-\infty)>A_{x}(+\infty)\end{cases} \tag{2}$$

with $A_x(-\infty)$ and $A_x(+\infty)$ constants. The peak electric field grows exponentially from the infinitely remote past in a first interval $\mathrm{I}=(-\infty,0]$ (switch-on at $t=-\infty$), reaches a maximum amplitude $E>0$ at $t=0$, and decreases exponentially to the infinitely remote future in a second interval $\mathrm{II}=(0,+\infty)$ (switch-off at $t=+\infty$). The field and its t-electric potential step are

$$E(t)=E\begin{cases}e^{k_{1}t},\ t\in\mathrm{I},\\ e^{-k_{2}t},\ t\in\mathrm{II},\end{cases}\quad A_{x}(t)=E\begin{cases}k_{1}^{-1}\left(-e^{k_{1}t}+1\right),\ t\in\mathrm{I},\\ k_{2}^{-1}\left(e^{-k_{2}t}-1\right),\ t\in\mathrm{II},\end{cases} \tag{3}$$

where k_1 and k_2 are positive constants with k_1^{-1} and k_2^{-1} representing scales of time duration for the increasing and decreasing phases of the electric field. The maximum amplitude E occurs in a very sharp time instant, namely, $t=0$, such that the limit $\lim_{t\to-0}\dot{E}(t)\neq\lim_{t\to+0}\dot{E}(t)$ is not defined. The field and its potential are depicted below in Fig. 1.

The peak electric field described by Eq. (3) admit exact consideration in the framework of QED with t-electric potential steps [18, 23]. It has been shown in our previous publications [26, 27] that the Dirac equation[2]

$$i\partial_{t}\psi(x)=H(t)\psi(x),\quad H(t)=\gamma^{0}(\gamma\boldsymbol{P}+m),$$

$$P_{x}=-i\partial_{x}-U(t),\quad \boldsymbol{P}_{\perp}=-i\nabla_{\perp},\quad U(t)=-eA_{x}(t) \tag{4}$$

can be integrated in terms of hypergeometric confluent functions (HCFs) [28, 29], where $\psi(x)$ is a $2^{[d/2]}$-component spinor ($[d/2]$ stands for the integer part of the ratio $d/2$), $\perp$ stands for spatial components perpendicular to the electric

---

[1] Greek indices refer to the Minkowski spacetime $\mu=0,...,D$, while Latin indices refer to the Euclidean space $i=1,...,D$. Here $d=D+1$ is the dimension of the spacetime. Bold letters represent Euclidean vectors such as $\boldsymbol{r}=x^{1},x^{2},...,x^{D}$. The Minkowski metric tensor is diagonal $\eta_{\mu\nu}=\mathrm{diag}(+1,-1,...,-1)$.

[2] The relativistic system of units ($(\hbar=c=1)$) is used in this paper.

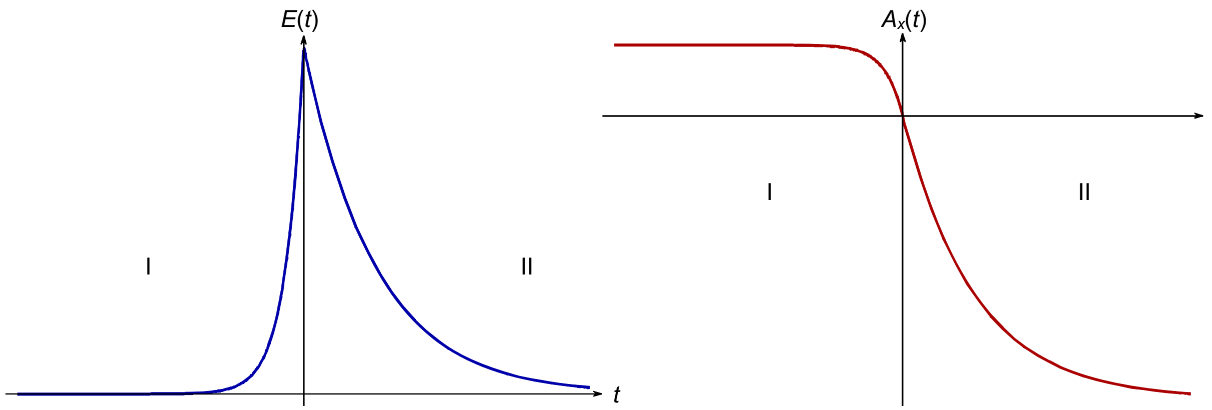

Fig. 1. Peak electric field $E(t)$ and its vector potential $A_x(t)$.

field, $m \neq 0$ is the electron mass, γ^μ are the γ-matrices in d dimensions, and $U(t)$ is the potential energy of one electron. Its exact solutions are represented as

$$\psi_n(x) = \exp(i\boldsymbol{pr})\psi_n(t), \quad n = (\boldsymbol{p}, \sigma),$$

$$\psi_n(t) = \left\{\gamma^0 i\partial_t - \gamma^1\left[p_x - U(t)\right] - \boldsymbol{\gamma p}_\perp + m\right\}\varphi_n(t) v_{\chi,\{\sigma\}} \tag{5}$$

in which $v_{\chi,\{\sigma\}}$ is a set of constant orthonormalized spinors $v^\dagger_{\chi,\{\sigma\}} v_{\chi',\{\sigma'\}} = \delta_{\chi,\chi'}\delta_{\{\sigma\},\{\sigma'\}}$ and $\varphi_n(t)$ are expressed in terms of HCFs $\Phi(a,c;\eta)$ as follows:

$$\varphi_n^j(t) = b_2^j y_1^j(\eta_j) + b_1^j y_2^j(\eta_j), \ y_1^j(\eta_j) = e^{-\eta_j/2}\eta_j^{\nu_j}\Phi(a_j, c_j; \eta_j),$$

$$y_2^j(\eta_j) = e^{\eta_j/2}\eta_j^{-\nu_j}\Phi(1-a_j, 2-c_j; -\eta_j). \tag{6}$$

Here the index j distinguishes quantities associated to the first I ($j=1$) from the second II ($j=2$) interval, respectively, b_1^j and b_2^j are constants fixed by the initial conditions, ν_j, a_j, and c_j constants, and η_j time-dependent functions

$$\nu_j = i\omega_j / k_j, \ \omega_j = \sqrt{\pi_j^2 + \pi_\perp^2}, \ \pi_j = p_x - (-1)^j eE/k_j, \ a_j = \frac{1}{2}(1+\chi) + (-1)^j i\pi_j/k_j + \nu_j, \ c_j = 1 + 2\nu_j,$$

$$\eta_1(t) = ih_1 e^{k_1 t}, \ \eta_2(t) = ih_2 e^{-k_2 t}, \ h_j = 2eE/k_j^2. \tag{7}$$

Selecting $\chi = 0$ in Eqs. (6) and (7) above allows one to discuss exact solutions for the Klein–Gordon (KG) equation.

By virtue of asymptotic properties of HCFs at $t \to \pm\infty$, one may classify functions (6) (and the corresponding Dirac spinors) according to their asymptotic behavior as plane waves at these limits. In this sense, we introduce an additional quantum number $\zeta = \pm$ to denote solutions corresponding to free-particle ($\zeta = +$) and antiparticle

($\zeta=-$) states at $t\to-\infty$ (${}_\zeta\varphi_n(t)$) and $t\to+\infty$ (${}^\zeta\varphi_n(t)$), respectively. More precisely, solutions (6) are conveniently written as

$$
{}_+\varphi_n(t)={}_+\mathcal{N}\exp(i\pi\nu_1/2)y_2^1(\eta_1),\ {}_-\varphi_n(t)={}_-\mathcal{N}\exp(-i\pi\nu_1/2)y_1^1(\eta_1),\ t\in\mathrm{I}\,,
$$

$$
{}^+\varphi_n(t)={}^+\mathcal{N}\exp(-i\pi\nu_2/2)y_1^2(\eta_2),\ {}^-\varphi_n(t)={}^-\mathcal{N}\exp(i\pi\nu_2/2)y_2^2(\eta_2),\ t\in\mathrm{II}\,, \tag{8}
$$

wherein ${}_\zeta\mathcal{N}$ and ${}^\zeta\mathcal{N}$ are normalization constants with respect to the inner product for Dirac spinors

$$
{}_\zeta\mathcal{N}={}_\zeta CV_{(d-1)}^{-1/2},\ {}^\zeta\mathcal{N}={}^\zeta CV_{(d-1)}^{-1/2},\ {}_\zeta C=\left(2\omega_1 q_1^\zeta\right)^{-1/2},\ {}^\zeta C=\left(2\omega_2 q_2^\zeta\right)^{-1/2},\ q_j^\zeta=\omega_j-\chi\zeta\pi_j\,, \tag{9}
$$

or for KG solutions

$$
{}_\zeta\mathcal{N}={}_\zeta\mathcal{C}V_{(d-1)}^{-1/2},\ {}^\zeta\mathcal{N}={}^\zeta\mathcal{C}V_{(d-1)}^{-1/2},\ {}_\zeta\mathcal{C}=(2\omega_1)^{-1/2},\ {}^\zeta\mathcal{C}=(2\omega_2)^{-1/2}\,, \tag{10}
$$

where $V_{(d-1)}$ is the spatial volume. For additional details concerning the structure of solutions, see [23, 26, 27].

2. DIFFERENTIAL AND TOTAL QUANTITIES

The most relevant objects in the study of particle creation by t-electric potential steps are decomposition coefficients between two pairs of complete and orthonormalized sets of exact solutions, namely, the in-$\left\{{}_\zeta\psi_n(x)\right\}$ and out-$\left\{{}^\zeta\psi_n(x)\right\}$ sets of Dirac spinors (or KG solutions). In the case under consideration, classification (8) allows us to express the out-set in terms of the in-set

$$
{}^\zeta\psi_n(x)={}_-\psi_n(x)g\left({}_-|^\zeta\right)+{}_+\psi_n(x)g\left({}_+|^\zeta\right) \tag{11}
$$

through certain coefficients $g\left({}_{\zeta'}|^\zeta\right)$ that are inner products between both sets of exact solutions[3]

$$
\left({}_{\zeta'}\psi_l,{}^\zeta\psi_n\right)=\delta_{l,n}g\left({}_{\zeta'}|^\zeta\right),\quad g\left({}^{\zeta'}|_\zeta\right)=g\left({}_{\zeta'}|^\zeta\right)^* \tag{12}
$$

and are diagonal matrix elements with respect to the quantum numbers $n=(\boldsymbol{p},\sigma)$, due to the structure of electric field (1). The importance behind these coefficients stems on the fact that they define linear canonical transformations between in- and out-sets of creation and annihilation operators

$$
a_n(\mathrm{in})=g({}_+|^+)a_n(\mathrm{out})+g({}_+|^-)b_n^\dagger(\mathrm{out})\,,\ \kappa b_n^\dagger(\mathrm{in})=g({}_-|^+)a_n(\mathrm{out})+g({}_-|^-)b_n^\dagger(\mathrm{out})\,, \tag{13}
$$

[3] The notation $\left(\psi',\psi\right)$ stands for inner products of Dirac spinors. For details, see [23, 30].

from which one may compute basic elements concerning particle creation, for instance, the differential mean number of particles created from the initial vacuum[4]

$$N_n^{\mathrm{cr}} = \left\langle 0,\mathrm{in}\left| a_n^\dagger(\mathrm{out}) a_n(\mathrm{out}) \right| 0,\mathrm{in} \right\rangle = \left| g\left({}_-|^+\right) \right|^2 , \tag{14}$$

the total number

$$N = \sum_n N_n^{\mathrm{cr}} = \sum_n \left| g\left({}_-|^+\right) \right|^2 = \frac{V_{(d-1)}}{(2\pi)^{d-1}} J_{(d)} \int d\boldsymbol{p}\, N_n^{\mathrm{cr}} , \tag{15}$$

and the vacuum-to-vacuum transition probability

$$P_v = \exp\left\{ \kappa \sum_n \ln\left[1 - \kappa N_n^{\mathrm{cr}}\right] \right\}. \tag{16}$$

In Eqs. (13) and (16), $\kappa = +1$ and $\kappa = -1$ refer to fermions and bosons[5], respectively. Moreover, the number $J_{(d)}$ in Eq. (15) denotes spinning degrees of freedom, such that $J_{(d)} = 2^{[d/2]-1}$ for fermions and $J_{(d)} = 1$ for bosons.

In [26] we derived the coefficient $g\left({}_-|^+\right)$ for the peak electric field expressed by Eq. (3) which for fermions takes the form

$$g\left({}_-|^+\right) = \mathcal{C}\Delta,\ \mathcal{C} = -\frac{1}{2}\sqrt{\frac{q_1^-}{\omega_1 q_2^+ \omega_2}} \exp\left[\frac{i\pi}{2}(\nu_1 - \nu_2)\right],$$

$$\Delta = \left[k_1 h_1 y_1^2(\eta_2) \frac{d}{d\eta_1} y_2^1(\eta_1) + k_2 h_2 y_2^1(\eta_1) \frac{d}{d\eta_2} y_1^2(\eta_2) \right]\Bigg|_{t=0} , \tag{17}$$

while for bosons reads

$$g\left({}_-|^+\right) = \mathcal{C}_{\mathrm{sc}}\, \Delta\big|_{\chi=0},\ \mathcal{C}_{\mathrm{sc}} = \left(4\omega_1\omega_2\right)^{-1/2} \exp\left[i\pi(\nu_1 - \nu_2)/2\right], \tag{18}$$

with Δ given by Eq. (17). Using these results, we present plots of the mean number of particles created from the vacuum (Eq. (14)) as a function of p_x for different values of k_1 and k_2 (Fig. 2) and amplitude E of the peak (Eq. (3), Fig. 3). For the sake of simplicity, we choose from now on a symmetrical field configuration $k_1 = k_2 = k$, set $\boldsymbol{p}_\perp = 0$, and select the reduced system of units[6] [ru], in which besides $\hbar = c = 1$ the particle mass is also set equal to unity, $m = 1$. In this system the Compton wavelength corresponds to one unit of length $\lambda_e = \hbar / mc = 1[\mathrm{ru}] \simeq 3.8614\times 10^{-14}$ m, one unit of time corresponds to $\lambda_e / c = 1[\mathrm{ru}] \simeq 1.3\times 10^{-21}$ s, and one

[4] Which coincides with the mean number of antiparticles created from the vacuum.
[5] By *bosons* we mean the *Klein–Gordon particles*.
[6] This system of units is convenient for numerical and exact calculations; for example, see [31].

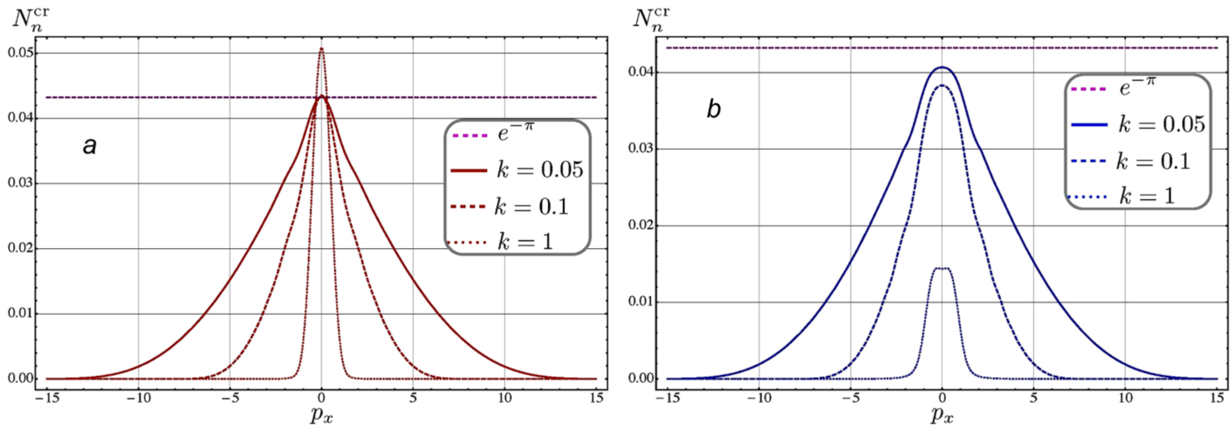

Fig. 2. Mean number of fermions (*a*) and bosons (*b*) created from the vacuum by a symmetrical peak electric field with amplitude $E = \varepsilon E_c$, where $\varepsilon = 1, 2$.

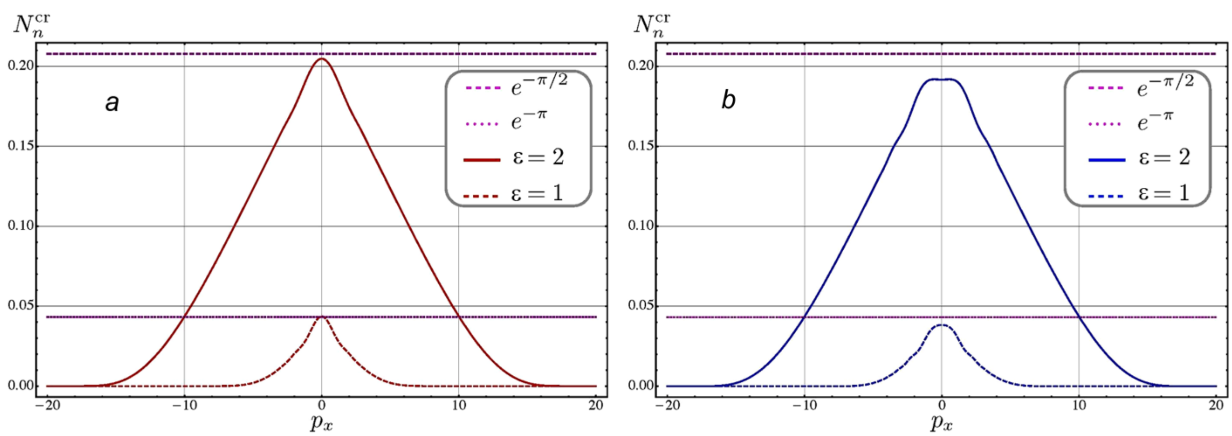

Fig. 3. Mean number of fermions (*a*) and bosons (*b*) created from the vacuum by a symmetrical peak electric field with amplitudes E equal to one (dashed curves) and critical fields corresponding to $\varepsilon = E / E_c = 1$ and $\varepsilon = 2$, respectively.

unit of energy corresponds to the electron rest energy $mc^2 = 1[\text{ru}] \simeq 0.511$ MeV. In all plots below, the longitudinal momentum p_x is relative to the electron mass m, that is, $p_x = p_x/m$ in the reduced system of units.

The results shown in Fig. 2 reveal wider distributions (solid curves) corresponding to peak electric fields with small values of k in comparison to those with higher values of this phase (dashed curves); feature that is common both for fermions and bosons. Since the inverse parameter k^{-1} represents a scale of time duration for increasing and decreasing phases, the results are consistent with the fact that the larger the duration of an electric field, the longer it has to accelerate pairs. Consequently larger values to p_x are expected in plots corresponding to electric fields with larger duration. In Fig. 3 similar results occur by keeping k fixed and varying the amplitude E. Larger distributions (solid curves) are associated with larger values to the amplitude E. Neglecting back reaction effects, the results displayed in Fig. 3 are consistent with the fact that larger electric fields produce more particles and, therefore, accelerate pairs with higher magnitudes.

Besides the characteristics above, it should be noted that the mean number of particles created tends to the uniform distribution $N_n^{cr} \to e^{-\pi\lambda}$ as k decreases (horizontal dashed lines in Figs. 2 and 3). In fact, this is in agreement

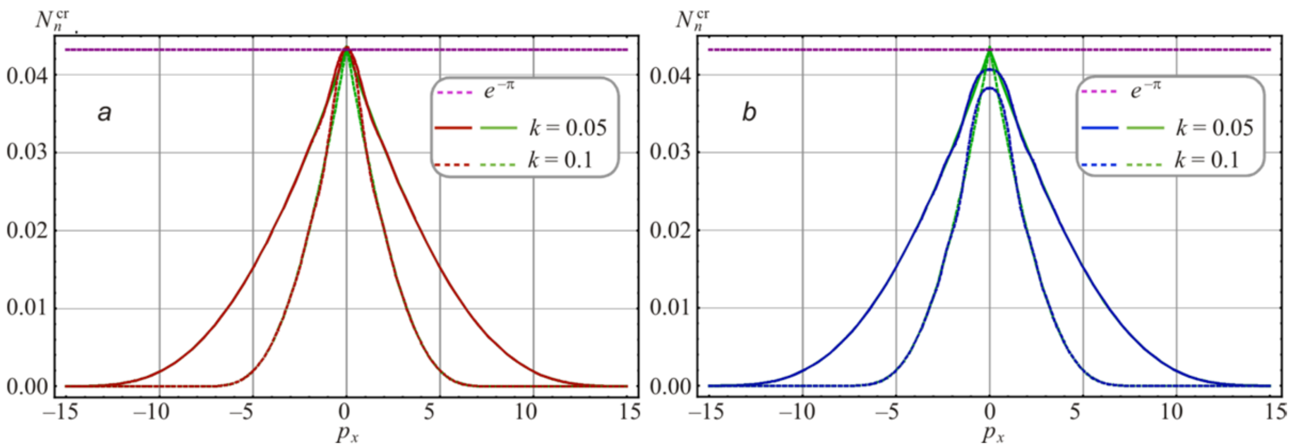

Fig. 4. Mean number of fermions (*a*) and bosons (*b*) created from the vacuum by a symmetrical peak electric field with amplitudes E equal to one critical field. Here exact results (bold curves) with asymptotic estimates (gray curves) are shown for two possible values of k, namely $k = 0.05$ (solid curves) and $k = 0.1$ (dashed curves).

with asymptotic calculations discussed by us before, in which the leading order term for the mean number with sufficiently small phases k_1 and k_2, satisfying

$$\min(h_1, h_2) \gg \max\left(1, m^2 / eE\right), \tag{19}$$

tends to the uniform distribution $e^{-\pi\lambda}$ (see Eqs. (3.7), (3.8) and (3.14) in [24]). This result is graphically illustrated above. Within conditions (19), we also discussed a range of sufficiently large values to p_x, in which the mean number of particles created from the vacuum acquires the asymptotic form

$$N_n^{cr} \approx \begin{cases} \exp\left[-2\pi\left(\omega_1 - \pi_1\right) / k_1\right], \; p_x < 0, \\ \exp\left[-2\pi\left(\omega_2 + \pi_2\right) / k_2\right], \; p_x > 0, \end{cases} \tag{20}$$

valid both for fermions and bosons. To illustrate this asymptotic limit, we show in Fig. 4 plots of exact expressions (15) for N_n^{cr} (solid and dashed curves for fermions and bosons, respectively) and asymptotic approximation (20) for different values of k, namely, $k = 0.05$ (solid curves) and $k = 0.1$ (dashed curves). Both values fulfill inequality (19), since $k = 0.05$ corresponds to $h_1 = h_2 = h = 2/k^2 = 800$ and $k = 0.1$ corresponds to $h = 200$. In both plots displayed in Fig. 4, it is seen a better approximation between exact and asymptotic results as p_x increases, as expected.

To discuss additional peculiarities, specially concerning total quantities, we perform numerical integration (using the program *Mathematica*) of the mean number of particles created (15) and (20), with respect to p_x, for several values of k. The results correspond to numerical values of the density of pairs created with zero perpendicular momentum $\mathbf{p}_\perp = 0$ normalized by the factor $J_{(d)}/(2\pi)^{d-1}$. It is worth to note that setting $p_\perp = 0$ is equivalent to a two-dimensional case $d = 2$, in which $J_{(2)} = 1$ for fermions. In [26] we calculated analytically the total number of particles created, by using asymptotic result (20) under conditions (19). Then we confront this approximation by comparing numerical estimates of both integrals. The results displayed in Fig. 5 reveal, indeed, that asymptotic expressions (20) are more accurate for peak electric fields with small values of k as expected. This is illustrated by

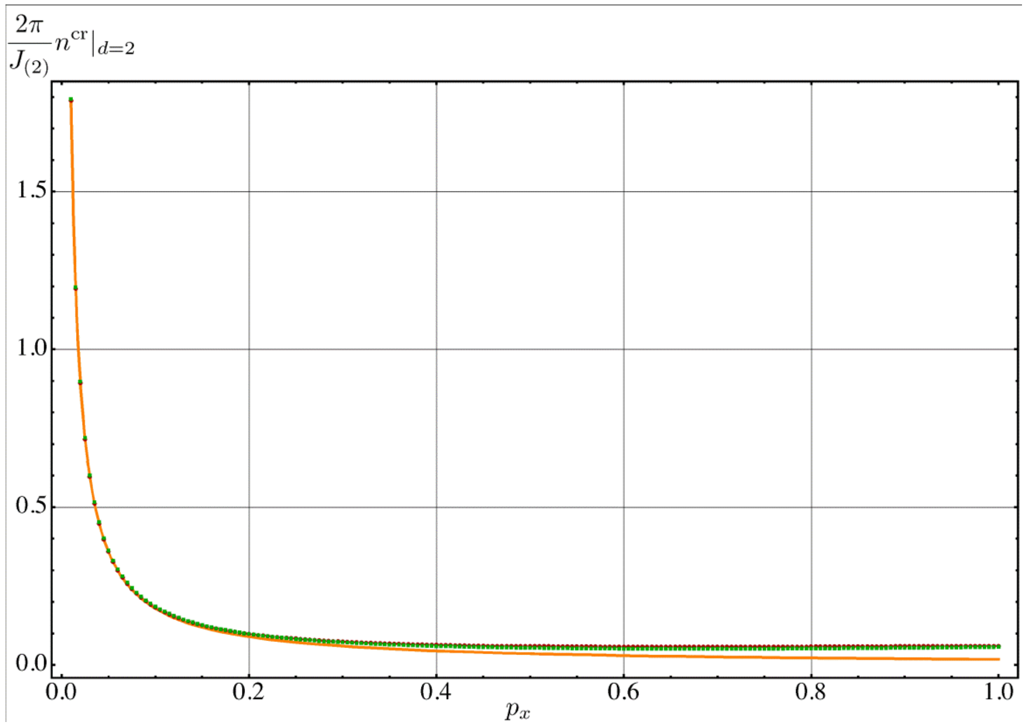

Fig. 5. Comparison between numerical and analytical results of the density of pairs created from the vacuum by a symmetrical peak field. Here circles correspond to numerical results of exact expressions (15), diamonds correspond to numerical results of Eq. (20), and the bold curve represents the analytical result proportional to k^{-1}, according to Eq. (23). Adjacent points are related by $k_{j+1} - k_j = 0.005$.

shorter distances between circles and diamonds for k approaching to zero, when compared to distances close to unity. Nevertheless, it should be noted that asymptotic form (20) provides a good approximation to exact expressions (15) in the range $0.01 \le k \le 1$ considered above. Moreover it is clearly seen that peak electric fields with small k (large time duration) produce more particles, due to higher values to the y-coordinate associated with small values for k.

The dependence on k displayed in Fig. 5 is still worth of consideration. In [24] we found that the total density of pairs created $n^{\mathrm{cr}} = N^{\mathrm{cr}}/V_{(d-1)}$ is given by

$$n^{\mathrm{cr}} = r^{\mathrm{cr}}\left(\frac{1}{k_1} + \frac{1}{k_2}\right) G\left(\frac{d}{2}, \pi\frac{m^2}{eE}\right), \quad r^{\mathrm{cr}} = \frac{J_{(d)}\left(eE\right)^{d/2}}{(2\pi)^{d-1}} \exp\left(-\pi\frac{m^2}{eE}\right), \tag{21}$$

where

$$G\left(\alpha, x\right) = \int_1^\infty \frac{ds}{s^{\alpha+1}} e^{-x(s-1)} = e^x x^\alpha \Gamma\left(-\alpha, x\right), \tag{22}$$

and $\Gamma\left(-\alpha, x\right)$ is the incomplete gamma function. Evaluating this density, normalized by $J_{(2)}/\left(2\pi\right)$, using the asymptotic expression (20) for the particular case $d = 2$ and $k_1 = k_2 = k$, one obtains

$$\frac{2\pi}{J_{(2)}} n^{\mathrm{cr}} \,|_{d=2} = 2\pi m^2 \Gamma\left(-1, \frac{\pi m^2}{eE}\right)\frac{1}{k}, \tag{23}$$

that is, the density of pairs created, as a function of k, behaves as k^{-1}. A comparison between this result (bold curves) and numerical ones (circles and diamonds) displayed in Fig. 5 illustrates a good approximation between analytical (23) and exact results in the range of values $0.01 \le k \le 1$, with higher accuracy for small values of k (slowly varying fields). Analogous agreement is observed for bosons. Therefore, analytical results provide a good approximation to describe the effect, when back reaction effects are ignored and specially in the slowly-varying regime.

3. FINAL COMMENTS

In this paper we summarized general aspects of vacuum instability by peak electric field in the framework of QED with t-electric potential steps and addressed to peculiarities of particle creation by such a field. To this end, we explored differential mean number of particles created from the vacuum and its dependence on the longitudinal momentum p_x for several symmetric field configurations, e. g., selecting different phases $k_1 = k_2 = k$ and amplitude E. In that respect it has been found wider distributions for peak fields with small phases k, as expected since k^{-1} correspond to time scale for the peak electric field and, therefore, the field has a larger time to accelerate pairs. Moreover, keeping phases fixed but changing the amplitude E, we found larger distributions for larger values of E; a common feature in cases where back reaction effects are ignored.

To understand how differential quantities depend on k, we compared exact and asymptotic expressions discussed before in [26] for some values of k. The comparison reveals asymptotic results more accurate at regions of sufficiently large p_x, whose accuracy increases as k decreases. Conversely, in the range of small p_x and k satisfying Eq. (19), the well-known uniform distribution $e^{-\pi\lambda}$ provides a better approximation instead, whose accuracy also increases as k decreases.

To extend the discussion, we explored the total density of pairs created and its dependence on k. To accomplish this analysis, we computed numerical integration of exact and asymptotic mean numbers with respect to p_x for several values of k. The results show that asymptotic expressions are more accurate for peak electric fields with small values of k, although asymptotic results provide a good approximation in the range $0.01 \le k \le 1$. To discuss the analytical dependence on k, we confront asymptotic analytical results with numerical calculations of exact expressions. In the range of values of k considered here, the k^{-1} dependence obtained from asymptotic expressions fits numerical estimates with a sufficient accuracy, which increases as k decreases.

The results presented in this article illustrate how a peak electric field create particles from the vacuum. The results are important to visualize how differential mean quantities depend on the quantum number p_x and, most of all, to compare with another exactly and non-exactly solvable models, with different time/space dependence and yet beyond the asymptotic regime, usually considered in slowly varying conditions. Comparing exact, numerical, and asymptotic results, we conclude that the total number of pairs created from the vacuum depend on k as k^{-1}, whose dependence is more accurate as k decreases. These results and those published recently by us in [26] provide a complete description of the process by the field in consideration.

This work was supported in part by the USA Energy Department (Contract DE-AC-02-76SF00515. SLAC-PUB-16913).

REFERENCES

1. O. Klein, Z. Phys., **53**, 157 (1929).
2. F. Sauter, Z. Phys., **69**, 742; **73**, 547 (1931).

3. W. Heisenberg and H. Euler, Z. Phys., **98**, 714 (1936).
4. F. Hund, Z. Phys., **117**, 1 (1940).
5. J. Schwinger, Phys. Rev., **82**, 664 (1951).
6. W. H. Furry, Phys. Rev., **81**, 115 (1951).
7. A. I. Nikishov, Zh. Eksp. Teor. Fiz., **57**, No. 4, 1210–12160 (1970).
8. N. B. Narozhnyi and A. I. Nikishov, Yad. Fiz., **11**, 1072 (1970).
9. A. I. Nikishov, Trudy FIAN SSSR, **111**, 153–271 (1979).
10. A. I. Nikishov, Nucl. Phys. B, **21**, 346 (1970).
11. A. I. Nikishov, Yad. Fiz., **67**, No. 8, 1503-1511 (2004); arXiv:hep-th/0111137.
12. A. I. Nikishov and V. I. Ritus, Zh. Eksp. Teor. Fiz., **46**, No. 2, 776–796 (1964); No. 5, 1768–1781 (1964).
13. N. B. Narozhnyi and A. I. Nikishov, Teor. Mat. Fiz., **26**, No. 1, 16–34 (1976).
14. E. Brezin and C. Itzykson, Phys. Rev. D, **2**, 1191 (1970).
15. V. S. Popov, Zh. Eksp. Teor. Fiz., **62**, No. 4, 1248–1262 (1972).
16. D. M. Gitman, J. Phys. A, **10**, 2007–2020 (1977).
17. E. S. Fradkin and D. M. Gitman, Fortschr. Phys., **29**, 381–411 (1981).
18. E. S. Fradkin, D. M. Gitman, and S. M. Shvartsman, Quantum Electrodynamics with Unstable Vacuum, Springer, Berlin (1991).
19. W. Greiner, B. Müller, and J. Rafelsky, Quantum Electrodynamics of Strong Fields, Springer, Berlin (1985).
20. N. D. Birrell and P. C. W. Davies, Quantum Fields in Curved Space, Cambridge University Press, Cambridge (1982).
21. A. A. Grib, S. G. Mamayev, V. M. Mostepanenko, Vacuum Quantum Effects in Strong Fields, Friedman Laboratory Publishing, Saint Petersburg (1994).
22. S. P. Gavrilov and D. M. Gitman, Phys. Rev. D, **53**, 7162–7175 (1996).
23. T. C. Adorno, S. P. Gavrilov, and D. M. Gitman, arXiv:1512.01288.
24. R. Ruffini, G. Vereshchagin, and S. Xue, Phys. Rep., **487**, 1–140 (2010).
25. F. Gelis and N. Tanji, Prog. Part. Nucl. Phys., **87**, 1–49 (2016).
26. T. C. Adorno, S. P. Gavrilov, and D. M. Gitman, Eur. Phys. J. C, **76**, 447 (1–15) (2016).
27. T. C. Adorno, S. P. Gavrilov, and D. M. Gitman, Physica Scripta, **90**, 074005 (1–8) (2015).
28. Higher Transcendental Functions (Bateman Manuscript Project), Vols. 1 and 2, A. Erdélyi *et al*., eds., McGraw-Hill, New York (1953).
29. NIST Digital Library of Mathematical Functions, http://dlmf.nist.gov/, 2015-08-07 DLMF Update; Version 1.0.10.
30. S. S. Schweber, An Introduction to Relativistic Quantum Fields, Dover Publications, Mineola, New York (2005).
31. I. A. Aleksandrov, G. Plunien, and V. M. Shabaev, Phys. Rev. D, **94**, 065024 (2016).